DOI: 10.1111/j.1541-0420.2005.00403.x

Detecting Pulsatile Hormone Secretions Using Nonlinear Mixed Effects Partial Spline Models

Yu-Chieh Yang,[1,*] **Anna Liu,**[2,**] **and Yuedong Wang**[3,***]

[1]Department of Statistics, National Taichung Institute of Technology, Taichung, Taiwan
[2]Department of Mathematics and Statistics, University of Massachusetts, Amherst, Massachusetts 01003, U.S.A.
[3]Department of Statistics and Applied Probability, University of California, Santa Barbara,
California 93106, U.S.A.
[*]*email:* yuchieh@ntit.edu.tw
[**]*email:* anna@math.umass.edu
[***]*email:* yuedong@pstat.ucsb.edu

Summary. Neuroendocrine ensembles communicate with their remote and proximal target cells via an intermittent pattern of chemical signaling. The identification of episodic releases of hormonal pulse signals constitutes a major emphasis of endocrine investigation. Estimating the number, temporal locations, secretion rate, and elimination rate from hormone concentration measurements is of critical importance in endocrinology. In this article, we propose a new flexible statistical method for pulse detection based on nonlinear mixed effects partial spline models. We model pulsatile secretions using biophysical models and investigate biological variation between pulses using random effects. Pooling information from different pulses provides more efficient and stable estimation for parameters of interest. We combine all nuisance parameters including a nonconstant basal secretion rate and biological variations into a baseline function that is modeled nonparametrically using smoothing splines. We develop model selection and parameter estimation methods for the general nonlinear mixed effects partial spline models and an R package for pulse detection and estimation. We evaluate performance and the benefit of shrinkage by simulations and apply our methods to data from a medical experiment.

Key words: Endocrinology; Hormone data; Model selection; Random effects; Semiparametric nonlinear mixed effects model; Shrinkage; Smoothing spline.

1. Introduction

Hormones play an important role in regulating biological processes. Through secretions of hormones, signals are sent to the other organs enabling interaction within the human body (Keener and Sneyd, 1998). There are two types of secretions: pulsatile secretions that are bursts of hormone from glands to bloodstream, and basal secretion that is a tonic pattern secretion (Merriam and Wachter, 1982; Keenan and Veldhuis, 1997; Guo, Wang, and Brown, 1999). Since pulses act as signals to target organs for physiological communication within the endocrine system, it is biologically and clinically important to investigate the occurrence and/or frequency of pulses. The identification of discrete hormonal pulse signals constitutes a major emphasis of endocrine investigation (Merriam and Wachter, 1982; Veldhuis and Johnson, 1986; Veldhuis, Carlson, and Johnson, 1987; O'Sullivan and O'Sullivan, 1988; Kushler and Brown, 1991; Guo et al., 1999; Johnson, 2003).

Experiments are typically conducted in such a way that some hormone concentrations are measured from blood samples withdrawn at regular time intervals, say every 10 minutes, for a period of time, say 24 hours, from a group of normal (or sick) human subjects (or animals). For example, in an experiment conducted at the University of Michigan, 10-minute sampling for hormones adrenocorticotropic (ACTH) and cortisol was performed for 24 hours in 36 patients with fibromyalgia and/or chronic fatigue syndrome and 36 age-matched controls (Crofford et al., 2004). Figure 1 shows the profile of ACTH concentrations over time from a patient. Pulse locations and a baseline function are estimated by the methods proposed in this article.

The goal of the study was to investigate disease effects, if any, on the secretion pattern. Statistical problems at the first stage of the data analysis are to estimate the number and locations of pulses, parameters such as the mass (amplitude) and half-life associated with each pulse, and the baseline (Crofford et al., 2004). These problems are technically challenging due to indirect observations, near confounding among several components, and multiple sources of variation. "There are many proposed pulse-detection algorithms, all based upon trying to detect a point of rapid increase, but none has proven to be completely acceptable" (Keenan, Sun, and Veldhuis, 2000).

Existing methods for pulse identification and characterization fall into two categories: criterion-based methods that use test statistics to identify rises and/or falls in hormone concentration, and model-based methods that assume statistical models to approximate the secretion pattern.

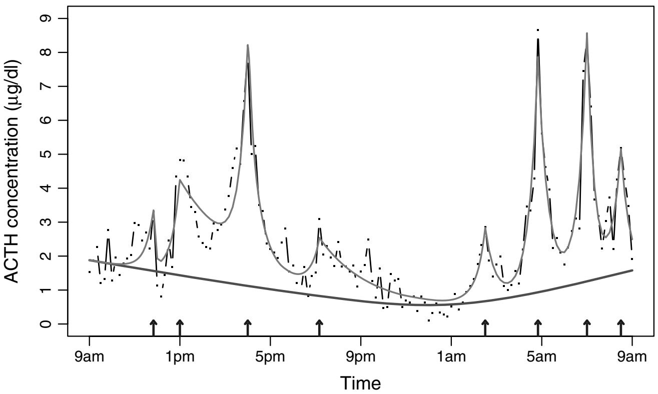

Figure 1. Profile of ACTH concentration of a patient with chronic fatigue syndrome (broken line). Pulse locations identified by our method with the BIC criterion are marked below as vertical arrows. The overall fit and estimated baseline function are plotted as solid lines.

Among criterion-based methods, CLUSTER compares the concentrations at a peak location with concentrations at the nearest nadir using a two-sample t-test (Veldhuis and Johnson, 1986). In general, most criterion-based methods use the assay's coefficient of variance (CV) as the true CV. Other sources of variation such as biological noises are ignored. Therefore estimates of quantities related to variation such as the threshold are biased, which leads to over-identifying the numbers of pulses. Among the model-based methods, Veldhuis et al. (1987) used a biophysical model that represents the hormone concentration as the convolution of a secretion rate with an elimination function (see Section 2.1 for more details). O'Sullivan and O'Sullivan (1988) represented the hormone concentration as a convolution of individual pulses with their locations following a nonhomogeneous Poisson process. Guo et al. (1999) proposed a state-space model that incorporates a nonconstant baseline. In general, the model-based methods are preferred to criterion-based methods based on the false positive and false negative error rates (Mauger, Brown, and Kushler, 1995). Model-based methods also provide estimates for the parameters of interest. Criterion-based methods are often used to identify initial pulses for model-based methods.

In this article, we propose nonlinear mixed effects partial spline models to detect pulse locations and estimate parameters. All current model-based methods except Guo et al. (1999) assume a constant or zero baseline. These restrictive assumptions may lead to biases in estimates of the parameters. We combine all nuisance parameters into a baseline function and model it nonparametrically using smoothing splines. All current model-based methods assume that parameters such as the decay rate are fixed and common for all pulses. Thus all these methods ignore biological variations between pulses within a subject which may be of scientific interest (Keenan et al., 2003; Keenan and Veldhuis, 2003). We introduce a general second-stage mixed effects model for parameters that allows us to model variation between pulses and incorporate covariate effects and/or feedback mechanisms. Pooling information from different pulses, our estimates have smaller mean-squared errors (MSE). We also allow random errors to be correlated. We develop an estimation procedure for a general form of pulse-shape function. Therefore, our methods and software can be applied to fit models with several different pulse-shape functions in the literature. Conditional on the number and locations of pulses, we estimate all parameters using methods developed in Ke and Wang (2001). We develop new model selection methods for estimating the number and locations of pulses. We also develop an R package to implement our estimation procedure.

The article is organized as follows. Section 2 introduces the nonlinear mixed effects partial spline model. Section 3 describes methods for pulse detection and parameter estimation. Section 4 presents simulation results. Section 5 presents the analysis of the data set introduced in Section 1. Section 6 concludes the article with a brief discussion.

2. Nonlinear Mixed Effects Partial Spline Model

2.1 *Biophysical Models for Hormonal Secretions and Measurements*

Usually observations are taken in a time period, typically 24 hours. Without loss of generality, we assume that the time period has been transformed into an interval [0, 1]. The secretion rate at time t can be represented by (Keenan and Veldhuis, 1997; Keenan et al., 2003)

$$S(t) = \rho(t) + \sum_{k=1}^{K} \alpha_k \psi(t - \tau_k), \tag{1}$$

where $\rho(t)$ is the rate of basal secretion, K is the number of pulsatile secretions and $\tau_1 < \tau_2 < \cdots < \tau_K$ are successive onset times, α_k is the mass of the kth pulse, and ψ is the waveform. Note that we allow a nonconstant basal secretion rate. Concentration at time t, $X(t)$, is (Keenan, Veldhuis, and Yang, 1998)

$$\begin{aligned} X(t) &= X(0)E(t) + \int_0^t S(u)E(t-u)\,du + g(t) \\ &= X(0)E(t) + \int_0^t \rho(u)E(t-u)\,du + g(t) \\ &\quad + \sum_{k=1}^{K} \alpha_k \int_0^t \psi(u - \tau_k)E(t-u)\,du, \end{aligned} \tag{2}$$

where $X(0)$ is the concentration at time 0, E is an elimination function, and g represents microscopic biological variation. The central part of the model is convolutions of pulse waveforms with elimination functions.

Observations measured from blood samples drawn at discrete time points are

$$y_j = X(t_j) + \epsilon_j, \quad j = 1, \ldots, n, \tag{3}$$

where ϵ_j are usually assumed to be independent normal with mean zero and a constant variance or a constant coefficient of variation. We allow random errors to be correlated in this article.

Technical challenges include: (1) the number and locations of onset times are not observed, and (2) two modes of secretions and eliminations are near confounded. Even for the special case with $X(0) = 0$, $g(t) = 0$, $\rho(t) = 0$, $\alpha_k = 1$, and the assumption that onset times follow a nonhomogeneous Poisson process with intensity function $h(t)$, the expected concentration, $E(X(t)) = \int_0^t (\int_0^u \psi(u-v)h(v)\,dv)E(t-u)du$, involves two layers of convolutions. Thus the estimation of the intensity function h involves two layers of deconvolutions where the filter functions ψ and E depend on unknown parameters. The one-layer deconvolution with a single known filter function is a well-known ill-posed problem (Wahba, 1990).

2.2 *Nonlinear Partial Spline Models*

All current methods except Guo et al. (1999) assume that the basal secretion rate $\rho(t)$ is a constant function. Some methods even require that $\rho(t) = 0$. We assume that $\rho(t)$ is a smooth function and treat it as a nuisance parameter. Keenan et al. (1998) used a one-fold integrated Wiener process to model microscopic biological variation g in (2) which is equivalent to a linear spline (Wahba, 1990). We note that both $X(0)$ and g are unknown. They are nuisance parameters and are ignored by most of the current methods. These restrictive assumptions and omissions may lead to large bias in estimates of the parameters. We combine all three nuisance parameters into a *baseline function*

$$f(t) = X(0)E(t) + \int_0^t \rho(u)E(t-u)\,du + g(t). \tag{4}$$

We then consider the following general class of nonlinear partial spline models

$$y_i = f(t_i) + \sum_{k=1}^{K} \alpha_k p(\boldsymbol{\gamma}_k; t_i - \tau_k) + \epsilon_i, \quad i = 1, \ldots, n, \tag{5}$$

where y_i is the concentration measurement at time t_i, f is the baseline function, $p(\boldsymbol{\gamma}; \cdot)$ is the *pulse-shape* function with parameters $\boldsymbol{\gamma}$, K is the number of pulses, α_k, $\boldsymbol{\gamma}_k$, and τ_k are the mass (or amplitude), pulse-shape parameters, and onset (or peak) times associated with the kth pulse, and ϵ_i's are random errors. We allow random errors to be correlated. Specifically, let $\boldsymbol{\epsilon} = (\epsilon_1,\ldots,\epsilon_n)^T$. We assume that $\boldsymbol{\epsilon} \sim N(0, \sigma^2\boldsymbol{\Lambda})$. We now discuss how to model the pulse shape p and the baseline function f.

We will consider general pulse-shape function p in our estimation procedure and software implementation. Several prototype pulse-shape functions are used in the literature. One simple and useful pulse-shape function is the following double exponential pulse function (O'Sullivan and O'Sullivan, 1988)

$$p(\gamma; t-\tau) = \begin{cases} \exp\{\gamma_1(t-\tau)\}, & t < \tau, \\ \exp\{-\gamma_2(t-\tau)\}, & t \geq \tau. \end{cases} \tag{6}$$

For the double exponential pulse function, τ_k and α_k represent the peak time and amplitude of the kth pulse. In practice the ability to distinguish between different pulse-shape functions is limited by the sampling rate. The double exponential pulse functions usually provide good approximations. Therefore, even though our methods apply to the general pulse functions, we use the double exponential pulse function in our simulations and data analysis.

As indicated in (4), the baseline function f combines all nuisance parameters. It is reasonable to assume that f varies slowly over time. However, it is usually difficult, if not impossible, to specify a parametric model for f. Thus we model it nonparametrically using a polynomial spline with the model space (Wahba, 1990; Green and Silverman, 1994)

$$W_m = \left\{ f : f, f', \ldots, f^{(m-1)} \text{ absolutely continuous}, \right.$$
$$\left. \int_0^1 \left(f^{(m)}\right)^2 dt < \infty \right\}. \tag{7}$$

Here $m = 2$ corresponds to the well-known cubic spline that is used in our simulations and data analysis. We note that our methods apply to general spline models defined in Wahba (1990).

2.3 *Mixed Effects Models for Parameters*

Keenan et al. (1998) provided biological justifications for modeling the mass parameter as random effects

$$\alpha_k = \beta_1 + b_k, \quad b_k \overset{iid}{\sim} N\left(0, \sigma_b^2\right), \tag{8}$$

where random effects b_k model the biological variation. To allow mass to depend on the preceding inter-pulse interval, we may add $\beta_2 \times (\tau_k - \tau_{k-1})$ in model (8) which assumes a constant rate of mass accumulation (Keenan et al., 1998, 2003). Pulses may also be modulated by circadian rhythms (Keenan and Veldhuis, 1997). Specifically, masses vary in a systematic circadian pattern. To quantify the underlying pulsatile secretion-generating mechanisms, we may add a simple periodic function such as $\beta_3 \sin 2\pi\tau_k + \beta_4 \cos 2\pi\tau_k$ to model (8).

All existing methods ignore variations in the shape parameters and assume that $\boldsymbol{\gamma}_k = \boldsymbol{\gamma}$ for all pulses within a subject. Recent studies indicate that $\boldsymbol{\gamma}_k$ may vary during the day (Keenan et al., 2003; Keenan and Veldhuis, 2003). It is of scientific interest to model the variation between pulses. Random effects models discussed above for the mass parameter can also be constructed similarly for $\boldsymbol{\gamma}_k$.

In this article, we consider a general second-stage model for the mass α_k and shape parameters $\boldsymbol{\gamma}_k$ which include models discussed above as special cases. Let $\boldsymbol{\alpha} = (\alpha_1,\ldots,\alpha_K)^T$, $\boldsymbol{\gamma} = (\boldsymbol{\gamma}_1^T,\ldots,\boldsymbol{\gamma}_K^T)^T$, and $\boldsymbol{\phi} = (\boldsymbol{\alpha}^T, \boldsymbol{\gamma}^T)^T$. Then, we assume the following linear mixed model for all parameters $\boldsymbol{\phi}$

$$\boldsymbol{\phi} = \boldsymbol{A\beta} + \boldsymbol{Bb}, \quad \boldsymbol{b} \sim N(\boldsymbol{0}, \sigma^2\boldsymbol{D}), \tag{9}$$

where $\boldsymbol{\beta}$ and $\boldsymbol{b}$ are fixed and random effects, and $\boldsymbol{A}$ and $\boldsymbol{B}$ are design matrices for the fixed and random effects, respectively.

3. Pulse Detection and Estimation

The nonlinear mixed effects partial spline model (NMPSM) is the combination of the first-stage model (5) and the second-stage model (9). Let $\boldsymbol{y} = (y_1, \ldots, y_n)^T$, $\boldsymbol{f} = (f(t_1), \ldots, f(t_n))^T$, and $\boldsymbol{\eta} = (\sum_{k=1}^K \alpha_k p(\boldsymbol{\gamma}_k; t_1 - \tau_k), \ldots, \sum_{k=1}^K \alpha_k p \times (\boldsymbol{\gamma}_k; t_n - \tau_k))^T$. Then the NMPSM can be written in a matrix form

$$\begin{aligned} \boldsymbol{y} &= \boldsymbol{f} + \boldsymbol{\eta} + \boldsymbol{\epsilon}, \quad \boldsymbol{\epsilon} \sim N(\boldsymbol{0}, \sigma^2\boldsymbol{\Lambda}), \\ \boldsymbol{\phi} &= \boldsymbol{A\beta} + \boldsymbol{Bb}, \quad \boldsymbol{b} \sim N(\boldsymbol{0}, \sigma^2\boldsymbol{D}). \end{aligned} \tag{10}$$

In the following we assume that $\boldsymbol{\Lambda}$ and $\boldsymbol{D}$ depend on an unknown parameter vector $\boldsymbol{\theta}$. We need to estimate the number of pulses K, pulse locations $\boldsymbol{\tau} = (\tau_1, \ldots, \tau_K)^T$, $\boldsymbol{\beta}$, f, $\boldsymbol{\theta}$, σ^2, and $\boldsymbol{b}$. Since the total number of parameters depends on the unknown parameter K, it is difficult to estimate all the parameters simultaneously. Our estimation procedure consists of two stages

- *pulse detection*: estimate K and $\boldsymbol{\tau}$.
- *parameter estimation*: conditional on the estimates of K and $\boldsymbol{\tau}$, estimate $\boldsymbol{\beta}$, f, $\boldsymbol{\theta}$, σ^2, and $\boldsymbol{b}$.

3.1 *Parameter Estimation and Inference*

We present the second stage of our estimation procedure first. At this stage, we assume that K and $\boldsymbol{\tau}$ are known and develop methods for estimating $\boldsymbol{\beta}$, f, $\boldsymbol{\theta}$, σ^2, and $\boldsymbol{b}$. The NMPSM (10) is a special case of the semiparametric nonlinear mixed effects models (SNMM) proposed in Ke and Wang (2001). Thus, the same estimation method can be used. Specifically, the estimation procedure iterates between two steps. At the first step, for fixed σ^2 and $\boldsymbol{\theta}$, we estimate $\boldsymbol{\beta}$, f, and $\boldsymbol{b}$ by minimizing the following double-penalized log-likelihood:

$$\min_{f \in W_m, \boldsymbol{\beta}, \boldsymbol{b}} \left\{ (\boldsymbol{y} - \boldsymbol{f} - \boldsymbol{\eta})^T \boldsymbol{\Lambda}^{-1} (\boldsymbol{y} - \boldsymbol{f} - \boldsymbol{\eta}) + b^T \boldsymbol{D}^{-1} \boldsymbol{b} \right.$$
$$\left. + n\lambda \int_0^1 \left(f^{(m)}(u)\right)^2 du \right\}, \qquad (11)$$

where the first two terms are the Laplace approximation to the log-likelihood of the NMPSM, the third term is a penalty to the roughness of the function f, and λ is a smoothing parameter that controls the trade-off between the goodness-of-fit and the smoothness of the function f. We choose λ using a data-adaptive criterion such as the generalized cross validation (GCV) and generalized maximum likelihood (GML) methods (Wahba, 1990; Ke and Wang, 2001; Wang and Ke, 2002).

At the second step, fixing $\boldsymbol{\beta}$, f, and $\boldsymbol{b}$ at their current estimates $\boldsymbol{\beta}_{-}$, f_{-}, and $\boldsymbol{b}_{-}$, we estimate $\boldsymbol{\theta}$ and σ^2 by maximizing the approximate profile-likelihood

$$\log|\sigma^2 \boldsymbol{V}_{-}| + \sigma^{-2}(\boldsymbol{y} - \boldsymbol{f}_{-} - \boldsymbol{\eta}_{-} + \boldsymbol{Z}_{-}\boldsymbol{b}_{-})^T \boldsymbol{V}_{-}^{-1}$$
$$\times (\boldsymbol{y} - \boldsymbol{f}_{-} - \boldsymbol{\eta}_{-} + \boldsymbol{Z}_{-}\boldsymbol{b}_{-}), \qquad (12)$$

where $\boldsymbol{V}_{-} = \boldsymbol{\Lambda} + \boldsymbol{Z}_{-}\boldsymbol{D}\ \boldsymbol{Z}^T{}_{-}$ and $\boldsymbol{Z}_{-} = \partial\boldsymbol{\eta}/\partial\boldsymbol{b}|_{\boldsymbol{\beta}_{-},\boldsymbol{b}_{-}}$. Detailed implementation of this procedure can be found in Ke and Wang (2001).

Inferences on parameters, random effects, and the nonparametric baseline function are based on a linear mixed effects partial spline approximation at convergence. Specifically, denote $\hat{\boldsymbol{\phi}}$ as the estimate of $\boldsymbol{\phi}$ and $\hat{\boldsymbol{X}} = \partial\eta/\partial\boldsymbol{\phi}|_{\hat{\boldsymbol{\phi}}}$. Then, at convergence, we approximate model (10) by $\boldsymbol{y} \approx \boldsymbol{f} + \eta(\hat{\boldsymbol{\phi}}) + \hat{\boldsymbol{X}}(\boldsymbol{\phi} - \hat{\boldsymbol{\phi}}) + \boldsymbol{\epsilon}$. Let $\tilde{\boldsymbol{y}} = \boldsymbol{y} - \eta(\hat{\boldsymbol{\phi}}) + \hat{\boldsymbol{X}}\hat{\boldsymbol{\phi}}$. Then, we approximate the original NMPSM (10) by the following linear mixed effects partial spline model:

$$\tilde{\boldsymbol{y}} = \boldsymbol{f} + \hat{\boldsymbol{X}}\boldsymbol{A}\boldsymbol{\beta} + \hat{\boldsymbol{X}}\boldsymbol{B}\boldsymbol{b} + \boldsymbol{\epsilon}. \qquad (13)$$

Combining the parametric fixed effects, $\hat{\boldsymbol{X}}\boldsymbol{A}\boldsymbol{\beta}$, with the bases of the null space of f, model (13) is a special case of the nonparametric mixed effects model in Wang (1998) and Wang and Ke (2002). Covariance matrices of the best linear unbiased prediction (BLUP) estimates given in Theorem 1 of Wang (1998) are used for inferences.

3.2 *Pulse Detection*

We now present the first stage of our estimation procedure. The number of pulses is never known in practice. We propose methods for estimating K and $\boldsymbol{\tau}$ in this subsection. This stage of our estimation procedure consists of two phases

phase 1: identify potential pulse locations.
phase 2: create a nested sequence by eliminating pulses one by one and then decide the final model.

At the first phase, we want to find all possible pulses and not be concerned with false identifications. Many detection methods are available in the endocrinology and statistical literature. One may use any existing pulse detection method such as the CLUSTER method (Veldhuis and Johnson, 1986). When pulse locations are peaks of the double exponential function (6), the mean function has change points in the first derivative at these positions. Thus, existing methods for detecting change points in the first derivative can also be used (Yang, 2002). Simulations (not shown) indicate that both CLUSTER and change points methods perform well. The change point method tends to have a smaller false negative rate. Therefore, it is used in our simulations and data analysis. Other methods such as wavelet and local polynomials may also be used (Yang, 2002). We note that users can always add or eliminate pulse locations at this phase based on visual inspection. More details, R functions, and examples can be found in Yang, Liu, and Wang (2004b).

Let the number of potential pulses identified in the first step be set as $K_{\max}$. Denote the minimal number of pulses as $K_{\min}$. A simple choice of $K_{\min}$ is zero. In phase 2, we create a nested sequence of pulse locations by fitting the NMPSM (10) and eliminating the least significant pulse location one by one from $K_{\max}$ to $K_{\min}$. We then select the final model using a model selection criterion.

We now discuss model selection methods involved in phase 2 in some detail. For a fixed K, $K_{\min} \leq K \leq K_{\max}$, we fit the NMPSM (10) using the method discussed in Section 3.1. We define t-statistics

$$t_k = \hat{\alpha}_k / \sqrt{\hat{\mathrm{var}}(\hat{\alpha}_k)}, \quad k = 1, \ldots, K,$$

where $\hat{\mathrm{var}}(\hat{\alpha}_k)$ is the approximate variance of $\hat{\alpha}_k$ after linearization. Specifically, we compute $\hat{\alpha}_k$ using Theorem 1 in Wang (1998) based on the approximated linear mixed effects partial spline model (13). We then eliminate the pulse location with the smallest $|t_k|$. Simulations in Section 4 indicate that this simple procedure works very well: false pulse locations are correctly eliminated before true pulse locations in most simulations.

Denote models corresponding to the resulting nested sequence of pulse locations as $\mathcal{M}_{K_{\min}}, \ldots, \mathcal{M}_{K_{\max}}$. We need to select the final model among this sequence of models. Model (5) contains two additive components: the nonparametric baseline function and the parametric pulses. Usually as K increases, the complexity of the parametric component increases while the complexity required for f decreases. Therefore both λ and K act as tuning parameters and they usually compensate each other. Although pulse locations of the sequence created in the first step are nested, $\mathcal{M}_{K_{\min}}, \ldots, \mathcal{M}_{K_{\max}}$ are not necessarily nested since λ are different for different K. Consequently, the residual sum of squares is not necessarily decreasing as K increases. We will select the final model using a model selection criterion such as the Akaike information criterion (AIC; Akaike, 1973), Bayesian information criterion (BIC; Schwarz, 1978), risk inflation criterion (RIC; Foster and George, 1994), and GCV (Craven and Wahba, 1979). To be able to use these model selection procedures, we need to define a measure of complexity for the model $\mathcal{M}_K, K = K_{\min}, \ldots, K_{\max}$. For an additive model, it is reasonable to take the addition of degrees of freedom for each component as a measure of complexity. However, when a selection procedure is involved in the estimation, extra degrees of freedom are required (Hinkley, 1971; Friedman and Silverman, 1989; Friedman, 1991; Luo and Wahba, 1997). Let $\tilde{\boldsymbol{H}}(\hat{\lambda})$ be the smoother matrix for the nonparametric function f where $\hat{\lambda}$ is an estimate of λ by the GCV or the GML method (Wahba, 1990; Wang and Ke, 2002). A commonly used measure of complexity for f is $\mathrm{tr}\tilde{\boldsymbol{H}}(\hat{\lambda})$. Let $df_P(K)$ be the number of parameters associated with pulses. As in Luo and Wahba (1997), we define an inflated degree of freedom (IDF) to account for the extra cost for selecting pulse locations. Specifically, we define the total degrees of freedom for $\mathcal{M}_K$ as

$$df_K \equiv \mathrm{tr}\tilde{\boldsymbol{H}}(\hat{\lambda}) + \mathrm{IDF} \times df_P(K). \tag{14}$$

Simulations show that a good choice of IDF is around 1.2; the same value is suggested in Luo and Wahba (1997). IDF = 1, that is no inflation, leads to poor performance.

Let $RSS(K)$ be the residual sum of squares of model $\mathcal{M}_K$. Note that $RSS(K)$ depends on both K and λ. For a fixed K, as discussed in Section 3.1, we estimate λ by a data-driven method such as the GCV or GML method. Therefore, $\hat{\lambda}$ depends on K and λ is essentially profiled in $RSS(K)$. Now consider the following selection criteria:

$$RSS(K) + a\sigma^2\, df_K, \tag{15}$$

where $a = 2$, $a = \log n$, and $a = 2\log df_{K_{\max}}$ correspond to the AIC, BIC, and RIC criteria, respectively. We estimate σ^2 based on the biggest model with $K = K_{\max}$. The GCV criterion is defined as

$$RSS(K)/(1 - df_K/n)^2.$$

Estimate of K is the minimizer of one of those criteria which also decides $\boldsymbol{\tau}$ and the final model. Simulations show that all four model selection procedures work very well. BIC and RIC perform slightly better.

3.3 *Algorithm*

Combining all steps in two stages, we have the following algorithm.

1. *Initialize*: identify potential pulse locations and provide initial values. Denote the total number of potential pulses as $K_{\max}$. Specify a low bound for the number of pulses $K_{\min}$.
2. *Pulse detection*:
   (a) For $K = K_{\max}, K_{\max} - 1, \ldots, K_{\min}$, repeat
      i. fit the model (10) and compute t-statistics t_k, $k = 1, \ldots, K$.
      ii. delete the location with the smallest $|t_k|$.
   (b) Select the final model using one of the AIC, BIC, RIC, and GCV criteria.
3. *Parameter estimation*: fit the final model.

We use the estimation methods for the general SNMM to accomplish step 3. However, the R function developed for fitting SNMM (Wang and Ke, 2002) cannot be applied directly due to the complicated structure of the parametric part in (10). Therefore, we developed a new user-friendly R package, `PULSE`, for hormone pulse detection and estimation. `PULSE` consists of three main functions, `pulini`, `puldet`, and `pulest`, for steps 1, 2, and 3, respectively. The manual of `PULSE` contains more details and examples. It can be downloaded from `http://www.pstat.ucsb.edu/faculty/yuedong/software.html`.

Due to the complexity of the NMPSM, there may be multiple local optimal solutions. Good initial values are critical to the performance of our algorithm. We have developed several methods and R functions for finding good initial values (Yang, 2002; Yang et al., 2004b).

When desirable, a fixed effect model can be assumed for all parameters $\boldsymbol{\phi}$. Then, the second-stage model (9) contains the fixed effects part only. Estimation and software can be developed similarly (Yang, 2002). R functions in the `PULSE` package allow parameters to be specified as fixed, random, or mixed. Even when $\boldsymbol{\phi}$ is considered as deterministic, it may be advantageous to estimate them using the penalized likelihood (11). For example, model (8) corresponds to shrinking α_k toward the common mean. Pooling data from different pulses, the resulting shrinkage estimates have smaller variances. This is especially important for the estimation of decay rates. Usually there are only a few observations on each pulse, which makes the maximum likelihood estimates of the decay rates unreliable. All existing methods are forced to assume a common decay rate for all pulses. Our simulations in Section 4 indicate that the shrinkage estimates are more efficient.

4. Simulation

4.1 *Performance of Pulse Detection*

In this subsection, we conduct simulations to evaluate the performance of our methods for pulse detection. We generate data from model (5) with $n = 144$, $t_i = i/n$, and $f(t) = 0.5 \cos(2\pi t) + 2$. We consider two choices for the number of pulses, K: $K = 5$ or $K = 10$. For a fixed K, we generate pulse locations according to a nonhomogeneous Poisson process with intensity function $\lambda(t) = 35(0.26 - (t - 0.5)^2)$. We use the double exponential function (6) as the pulse-shape function with a fixed infusion rate, $\gamma_1 = 100$, and random amplitudes α_k and random decay rates γ_{2k}. Specifically, we generate pulse amplitudes such that $\log\alpha_k \overset{iid}{\sim} N(1, \sigma_1^2)$ and pulse decay rates such that $\log\gamma_{2k} \overset{iid}{\sim} N(3.66, \sigma_2^2)$. We generate random errors according to $\epsilon_i \overset{iid}{\sim} N(0, \sigma^2)$. We consider four settings for variance parameters σ, σ_1, and σ_2: (I) (σ, σ_1, σ_2) = (0.3, 0.3, 0.18); (II)(σ, σ_1, σ_2) = (0.5, 0.3, 0.18); (III) (σ, σ_1, σ_2) = (0.3, 0.5, 0.27); and (IV) (σ, σ_1, σ_2) = (0.5, 0.5, 0.27). We repeat 100 times for each simulation setting.

We use the change point method to identify initial pulse locations and then apply our elimination procedure with $K_{\min} = K/2$. We assume the second-stage models $\log\alpha_k \overset{iid}{\sim} N(\beta_1, \sigma_\alpha^2)$ and $\log\gamma_{2k} \overset{iid}{\sim} N(\beta_2, \sigma_{\gamma_2}^2)$. Note that instead of using model (8) which was assumed in Keenan et al. (1998), we use log transformations to relax positive constraints on α_k and γ_{2k}. For $K = 10$ and setting III, Figure 2 shows profiles of the AIC, GCV, BIC, and RIC criteria with IDF = 1.2

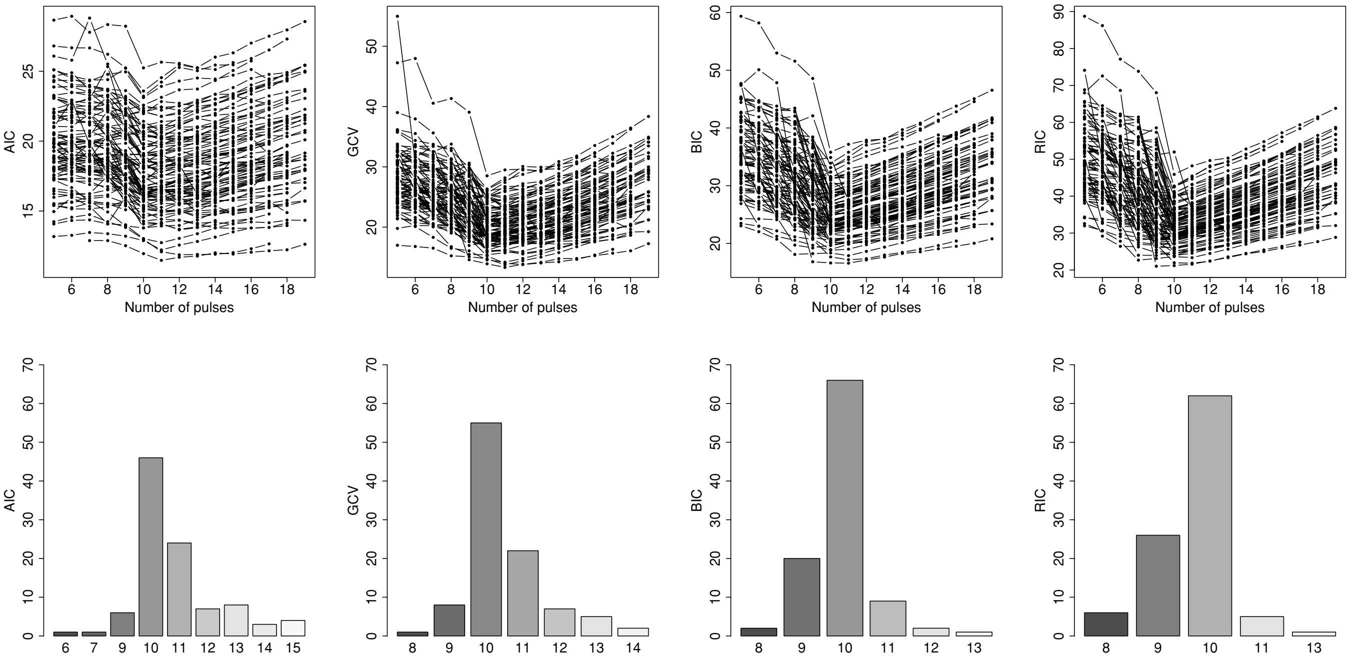

Figure 2. Four columns correspond to the AIC, GCV, BIC, and RIC criteria. The upper panel plots scores of these four criteria versus the number of pulses. The lower panel plots histograms of the estimated K.

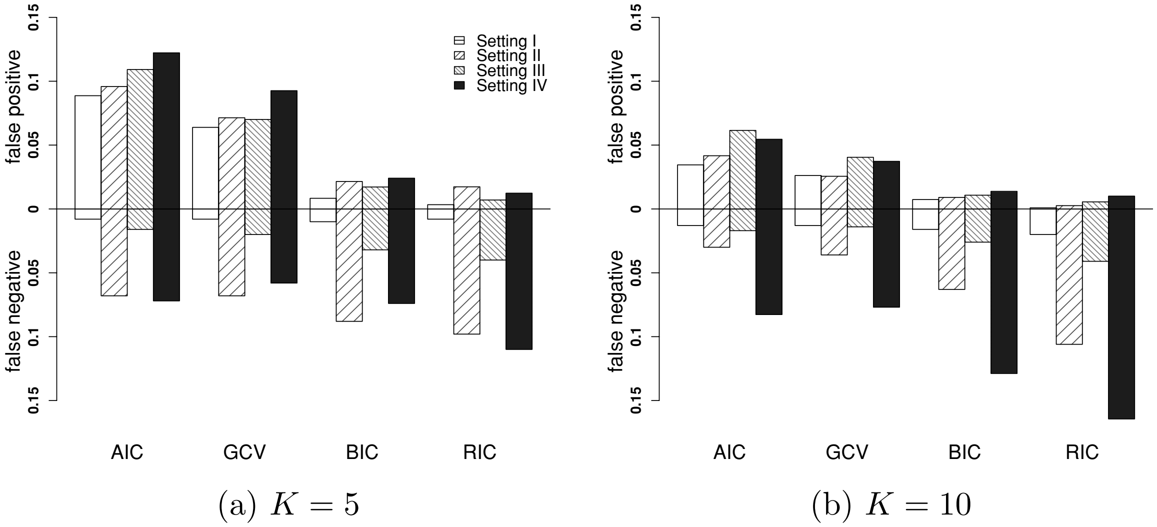

(a) $K = 5$

(b) $K = 10$

Figure 3. False positive and false negative rates.

and histograms of the estimated K based on these four criteria. Plots for other simulation settings are similar. Figure 3 plots the false positive rates and false negative rates for each setting. All four criteria provide good estimates of pulse numbers and pulse locations while BIC and RIC perform slightly better except for setting IV where variances are large. The performance depends on the choice of IDF: a larger IDF may improve the performance of the AIC and GCV. Overall, we recommend BIC and RIC with IDF = 1.2. We note that the performances of our methods in terms of false positive rates and false negative rates are comparable to those in Mauger et al. (1995) even though our simulation settings are more difficult with a slower sampling rate, multiple sources of variations, and a nonconstant baseline.

We treat the baseline function f as a nuisance parameter. Nevertheless, MSEs of $\hat{f}$ (not shown) indicate that our methods estimate the baseline function very well. See Yang, Liu, and Wang (2004a) for more references and simulation results.

4.2 *Efficiency of Shrinkage Estimates*

For linear regression models, it is well known that the shrinkage (also known as ridge) estimators reduce variance while increasing bias. With the right amount of shrinkage, it is always possible to reduce the MSE (Efron and Morris, 1975;

Table 1
MSEs and efficiencies of the estimates for the amplitudes and decay rates

Number of pulses	Parameters	Setting	Shrinkage	Standard	Efficiency
K = 5	Amplitudes	I	0.06	0.09	1.55
		II	0.14	0.22	1.62
		III	0.10	0.14	1.38
		IV	0.18	0.25	1.37
	Decay rates	I	0.12	0.42	3.52
		II	0.32	1.17	3.66
		III	0.20	0.67	3.41
		IV	0.30	1.28	4.22
K = 10	Amplitudes	I	0.15	0.45	3.00
		II	0.32	0.88	2.72
		III	0.23	0.59	2.55
		IV	2.73	4.24	1.55
	Decay rates	I	0.26	2.23	8.61
		II	0.50	3.82	7.65
		III	0.41	2.23	5.45
		IV	1.75	10.51	6.02

Gruber, 1998). In this section, we evaluate performance of the shrinkage methods for our nonlinear models. The simulation settings are the same as in Section 4.1. Instead of estimating the pulse locations, we now use true pulse locations and evaluate our estimation methods.

In this subsection we consider all parameters including α_k and γ_{2k} as deterministic and our estimates based on the NMPSM as the shrinkage estimates. Specifically, the shrinkage estimates are minimizers of the following penalized least squares:

$$||\boldsymbol{y} - \boldsymbol{f} - \boldsymbol{\eta}||^2 + \lambda_1 \sum_{k=1}^{K} (\log \alpha_k - \bar{\beta}_1)^2 + \lambda_2 \sum_{k=1}^{K} (\log \gamma_{2k} - \bar{\beta}_2)^2 + n\lambda \int_0^1 \left(f^{(m)}(u)\right)^2 du, \qquad (16)$$

where $\bar{\beta}_1 = \sum_{k=1}^{K} \log \alpha_k / K$, $\bar{\beta}_2 = \sum_{k=1}^{K} \log \gamma_{2k}/K$, and λ_1 and λ_2 are two shrinkage parameters. We shrink $\log \alpha_k$ and $\log \gamma_{2k}$ toward their grand means. Now consider a nonlinear mixed effect model with (5) as the first-stage model and random effects $\log \alpha_k \overset{iid}{\sim} N(\beta_1, \sigma^2/\lambda_1)$ and $\log \gamma_{2k} \overset{iid}{\sim} N(\beta_2, \sigma^2/\lambda_2)$. Then, it is not difficult to check that the penalized least squares (16) is equivalent to the penalized likelihood (11) with $\bar{\beta}_1$ and $\bar{\beta}_2$ replaced by β_1 and β_2. Therefore, we approximate the shrinkage estimates by the estimates of the corresponding nonlinear mixed effects model.

For comparison, we also calculate the least squares (LS) estimates of α_k and γ_{2k} using the `gnls` function in the `nlme` package. We repeat the simulation 100 times. Define MSE of $\hat{\alpha}_k$ as MSE $= \sum_{s=1}^{S} \sum_{k=1}^{K} (\hat{\alpha}_k^{(s)} - \alpha_k^{(s)})^2/(SK)$, where $\hat{\alpha}_k^{(s)}$ are the LS or shrinkage estimates of the true parameters $\alpha_k^{(s)}$ in the sth simulation and S is the number of simulations. The MSEs of $\hat{\gamma}_{2k}$ are defined similarly. Table 1 lists the MSEs of the LS and shrinkage estimates of α_k and γ_{2k}. The efficiencies, ratios between the MSE of the LS estimates and the MSE of the shrinkage estimates (Efron and Morris, 1975), are also listed in Table 1. Shrinkage estimators are obviously more efficient, especially for the decay rates. From our experiments, the comparative superiority becomes less obvious when the variation of a parameter becomes larger or error variance becomes smaller.

5. Application

We now show the analysis of the data introduced in Section 1. We used the double exponential function (6) to

Table 2
Summary of the elimination procedure and criteria scores. The column DROP lists initial locations eliminated at each iteration. DF is defined in equation (14) *with IDF* = 1.2.

Number of pulses	BIC	RIC	AIC	GCV	DROP	*DF*
13	82.673	106.897	52.847	62.965	10:30 PM	40.334
12	80.275	102.983	52.316	61.358	9:50 AM	37.809
11	78.252	99.593	51.975	60.219	9:20 PM	35.534
10	76.133	96.032	51.631	59.087	5:40 PM	33.134
9	73.760	90.818	52.757	59.767	11:00 AM	28.402
8	72.349	87.297	53.945	60.596	7:10 PM	24.889
7	73.652	89.228	54.475	61.680	11:50 AM	25.934
6	75.068	89.202	57.666	65.513	2:30 AM	23.534
5	79.926	92.618	64.298	73.722	1:00 PM	21.134

Table 3
Estimates of α_k and $\gamma_{2\mathrm{k}}$ on log scale and their standard errors

Location	α_k	SE	γ_{2k}	SE
11:50 AM	0.641	0.056	5.770	0.496
1:00 PM	1.074	0.012	2.272	0.076
4:00 PM	1.827	0.005	4.003	0.023
7:10 PM	0.458	0.041	2.632	0.172
2:30 AM	0.801	0.040	4.038	0.140
4:50 AM	1.934	0.004	3.961	0.021
7:00 AM	1.987	0.005	4.268	0.026
8:30 AM	1.351	0.028	4.117	0.113

model the pulse-shape function and a cubic spline to model the baseline function. Amplitudes and pulse decay rates are modeled using random effects. Specifically, we assume that $\log \alpha_k \overset{iid}{\sim} N(\beta_1, \sigma_\alpha^2)$, $\log \gamma_{2k} \overset{iid}{\sim} N(\beta_2, \sigma_{\gamma_2}^2)$, and they are mutually independent.

The change point method identified $K_{\max} = 13$ and potential pulse locations at 9:50 AM, 11:00 AM, 11:50 AM, 1:00 PM, 4:00 PM, 5:40 PM, 7:10 PM, 9:20 PM, 10:30 PM, 2:30 AM, 4:50 AM, 7:00 AM, and 8:30 AM. We then applied our elimination procedure with $K_{\min} = 5$. Table 2 shows the resulting sequence of pulse locations that are eliminated one by one. The estimates of the number of pulses based on the BIC, RIC, AIC, and GCV criteria are 8, 8, 10, and 10, respectively. The identified pulse locations using BIC, overall fit, and estimate of the baseline are shown in Figure 1. Table 3 lists estimates of the amplitudes and decay rates based on the final model selected by the BIC criterion.

6. Discussion

The NMPSM provides more efficient and stable estimates of parameters by allowing different shape parameters for pulses within each subject and combining all nuisance parameters into a baseline function. The general form of the second-stage mixed effects model will also allow researchers to investigate patterns of biological variation including circadian rhythms and feedback/feedforward control mechanisms (Keenan et al., 2003; Keenan and Veldhuis, 2003). The challenge lies in detecting the number and locations of pulses masked by indirect observations and multiple sources of variations. It requires a sophisticated model selection procedure such as the one proposed in this article.

Like all existing methods in the literature, our procedure in this article detects hormone pulses for each subject separately. Variations between subjects are usually accounted for in the second-stage analysis. One of our future research topics is to construct integrated models for all subjects, which will allow us to model both variations between subjects and variations between pulses within a subject.

We limited our discussions to the problem of hormone pulse detection. However, as a general model, the NMPSM has other potential applications when observations are in a form of signals plus slow changing baseline (Hunt, 1998; McBride, 2002; Yang, 2002). With slight modifications, our methods can be applied to these situations.

Acknowledgements

This research was supported by NIH grant R01 GM58533. The authors would like to thank Leslie J. Crofford, MD, and Professor Morton B. Brown from the University of Michigan for allowing us to use the hormone data. The authors thank the editor, the associate editor, and referee for their constructive comments and suggestions.

References

Akaike, H. (1973). Information theory and the maximum likelihood principle. In *International Symposium on Information Theory*, V. Petrov and F. Csáki (eds), 267–281. Budapest: Akademiai Kiádo.

Craven, P. and Wahba, G. (1979). Smoothing noisy data with spline functions. *Numerische Mathematik* **31,** 377–403.

Crofford, L. J., Young, E. A., Engleberg, N. C., Korszun, A., Brucksch, C. B., McClure, L. A., Brown, M. B., and Demitrack, M. (2004). Basal circadian and pulsatile ACTH and cortisol secretion in patients with fibromyalgia and/or chronic fatigue syndrome. *Brain, Behavior and Immunity* **18,** 314–325.

Efron, B. and Morris, C. (1975). Data analysis using Stein's estimator and its generalizations. *Journal of the American Statistical Association* **70,** 311–319.

Foster, D. P. and George, E. I. (1994). The risk inflation criterion for multiple regression. *Annals of Statistics* **22,** 1947–1975.

Friedman, J. H. (1991). Multivariate adaptive regression splines (with discussion). *Annals of Statistics* **19,** 1–67.

Friedman, J. H. and Silverman, B. W. (1989). Flexible parsimonious smoothing and additive modeling (with discussion). *Technometrics* **31,** 3–39.

Green, P. J. and Silverman, B. W. (1994). *Nonparametric Regression and Generalized Linear Models: A Roughness Penalty Approach.* London: Chapman and Hall.

Gruber, M. H. J. (1998). *Improving Efficiency by Shrinkage.* New York: Marcel Dekker.

Guo, W., Wang, Y., and Brown, M. B. (1999). A multiprocess state-space model for time series with pulse and changing baseline. *Journal of the American Statistical Association* **94,** 746–756.

Hinkley, D. (1971). Inference in two-phase regression. *Journal of the American Statistical Association* **66,** 736–743.

Hunt, M. A. (1998). Quantitative pattern recognition and non-linear model based analysis. Ph.D. Thesis, The University of Tennessee, Knoxville.

Johnson, T. D. (2003). Bayesian deconvolution analysis of pulsatile hormone concentration profiles. *Biometrics* **59,** 650–660.

Ke, C. and Wang, Y. (2001). Semi-parametric nonlinear mixed effects models and their applications (with discussion). *Journal of the American Statistical Association* **96,** 1272–1298.

Keenan, D. M. and Veldhuis, J. D. (1997). Stochastic model of admixed basal and pulsatile hormone secretion as modulated by a deterministic oscillator. *American Journal of Physiology (Regulatory, Integrative and Comparative Physiology 42)* **273,** R1173–R1181.

Keenan, D. M. and Veldhuis, J. D. (2003). Cortisol feedback state governs adrenocorticotropin secretory-burst shapes, frequency, and mass in a dual-waveform construct: Time of day-dependent regulation. *American Journal of Physiology* **285,** R950–R961.

Keenan, D. M., Veldhuis, J. D., and Yang, R. (1998). Joint recovery of pulsatile and basal hormone secretion by stochastic nonlinear random-effects analysis. *American Journal of Physiology* **275,** R1939–R1949.

Keenan, D. M., Sun, W., and Veldhuis, J. D. (2000). A stochastic biomathematical model of the male reproductive hormone system. *SIAM Journal on Applied Mathematics* **61,** 934–965.

Keenan, D. M., Roelfsema, F., Biermasz, N., and Veldhuis, J. D. (2003). Physiological control of pituitary hormone secretory-burst mass, frequency, and waveform: A statistical formulation and analysis. *American Journal of Physiology* **285,** R664–R673.

Keener, J. and Sneyd, J. (1998). *Mathematical Physiology.* New York: Springer.

Kushler, R. H. and Brown, M. B. (1991). A model for identification of hormone pulses. *Statistics in Medicine* **10,** 329–340.

Luo, Z. and Wahba, G. (1997). Hybrid adaptive splines. *Journal of the American Statistical Association* **92,** 107–116.

Mauger, D. T., Brown, M. B., and Kushler, R. H. (1995). A comparison of methods that characterize pulses in a time series. *Statistics in Medicine* **14,** 311–325.

McBride, S. J. (2002). A marked point process model for the source proximity effect in the indoor environment. *Journal of the American Statistical Association* **97,** 683–691.

Merriam, G. R. and Wachter, K. W. (1982). Algorithms for the study of episodic hormone secretion. *American Journal of Physiology* **243,** E310–E318.

O'Sullivan, F. and O'Sullivan, J. (1988). Deconvolution of episodic hormone data: An analysis of the role of season on the onset of puberty in cows. *Biometrics* **44,** 339–353.

Schwarz, G. (1978). Estimating the dimension of a model. *Annals of Statistics* **12,** 1215–1231.

Veldhuis, J. D. and Johnson, M. L. (1986). Cluster analysis: A simple versatile and robust algorithm for endocrine pulse detection. *American Journal of Physiology* **250,** E486–E493.

Veldhuis, J. D., Carlson, M. L., and Johnson, M. L. (1987). The pituitary gland secretes in bursts: Appraising the nature of glandular secretory impulses by simultaneous multiple-parameter deconvolution of plasma hormone concentration. *Proceedings of the National Academy of Science USA* **84,** 7686–7690.

Wahba, G. (1990). *Spline Models for Observational Data.* SIAM, Philadelphia. CBMS-NSF Regional Conference Series in Applied Mathematics, Vol. 59.

Wang, Y. (1998). Mixed-effects smoothing spline ANOVA. *Journal of the Royal Statistical Society Series B* **60,** 159–174.

Wang, Y. and Ke, C. (2002). ASSIST: A suite of S-plus functions implementing spline smoothing techniques. Manual for the ASSIST package. Available at `http://www.pstat.ucsb.edu/faculty/yuedong/software`.

Yang, Y. (2002). Detecting change points and hormone pulses using partial spline models. Ph.D. Thesis, University of California–Santa Barbara, Department of Statistics and Applied Probability.

Yang, Y., Liu, A., and Wang, Y. (2004a). *Detecting pulsatile hormone secretions using nonlinear mixed effects partial spline models.* Technical Report 399, Department of Statistics and Applied Probability, University of California–Santa Barbara. Available at `http://www.pstat.ucsb.edu/faculty/yuedong/research`.

Yang, Y., Liu, A., and Wang, Y. (2004b). PULSE: A suite of R functions for detecting pulsatile hormone secretions. Manual for the PULSE package. Available at `http://www.pstat.ucsb.edu/faculty/yuedong/software`.

Received September 2004. *Revised March* 2005.
Accepted April 2005.